ISSN 0005-1179 (print), ISSN 1608-3032 (online), Automation and Remote Control, 2025, Vol. 86, No. 2, pp. 153–164.

CONTROL IN TECHNICAL SYSTEMS

Approaches to Optimizing Guidance Methods to High-Speed Intensively Maneuvering Targets. Part III. Guidance Optimization Considering the Dynamic Properties of Interceptors

V. S. Verba[*,a], **V. I. Merkulov**[*,b], **and A. R. Ilchuk**[**,c]

[*] *JSC Concern Vega, Moscow, Russia*
[**] *LLC NPO Istok, Fryazino, Russia*
e-mail: [a] *vvs.msk@gmail.com,* [b] *mvipost41@gmail.com,* [c] *arilchuk@istokmw.ru*

Received March 20, 2024
Revised July 8, 2024
Accepted September 2, 2024

Abstract—Procedures for designing guidance methods to an object with a complex maneuvering law are considered. These procedures are adapted to the interceptor's dynamic properties, implemented by transforming the composition of information support and using the predicted spatial position of the target. Modeling results are presented.

Keywords: guidance method, control optimization, information support transformation, target position prediction

DOI: 10.31857/S0005117925020044

1. INTRODUCTION

According to an analysis of conventional guidance methods [1–4], with proportional guidance and predicted meeting point guidance as the most common ones, they were designed autonomously without considering the dynamic properties of aircraft interceptors for a non-maneuvering target.

When implementing interception systems for non-maneuvering and weakly maneuvering targets, such an approach imposes no significant constraints on the properties of aircraft interceptors (except for the maximum allowable overload). However, in the case of intensively maneuvering targets, this approach does not ensure the desired intercept performance, requiring an appropriate improvement of the maneuvering properties of an aircraft interceptor by adapting them to the complex nature of changes in the target's relative and absolute motion coordinates.

In turn, this leads to appreciable time and material costs and hence cannot be a universal technique due to the wide range of possible target maneuvers.

Therefore, there is a high demand for developing optimization methods considering the dynamic properties of interceptors.

The topicality of this problem grows with expanding the class of high-speed aircraft with complex maneuvering laws, including those with changes in the absolute value and signs of the derivatives of angular coordinates [4]. In this regard, it is necessary to develop optimization methods for generating control laws considering the dynamic properties of interceptors [5, 6, 8, 9].

In general, the interceptor's delay can be considered in various ways:

- by weighting the control error coefficients in accordance with the carrier's time constant and the gain of its control signals, which is characteristic of classical optimization methods in the statistical theory of optimal control (STOC) [5, 6];
- by describing the mismatch between the dynamic properties of the target and interceptor directly in the guidance law [5, 6];
- by forming guidance laws with a nonlinear (cubic) dependence on control error combinations that indirectly include the carrier's delay [5, 6];
- by transforming the input signals acting on the carrier to optimize its particular type and expand the number of corrections;
- by forming a guidance law based on predicting the target position for a time interval determined by the carrier's delay.

Note that the first three ways were discussed in detail in [5, 6].

This paper aims to consider optimization methods based on transforming input signals and using the predicted spatial position of the target.

2. OPTIMIZATION OF GUIDANCE METHODS BASED ON INPUT SIGNAL TRANSFORMATION

Here, the core consists in artificially increasing the number of corrective input signals that compensate for delay, to a greater or lesser extent, for an interceptor with particular flight characteristics.

Such a framework requires changes only in information support algorithms, without affecting the aircraft interceptor.

Note that the required transformation of input signals for guidance system optimization can be obtained by using STOC algorithms [1, 3].

Consider the simplest form of this approach, based on local optimization [1]. For a given system (interceptor) described by

$$\dot{\mathbf{x}}_{\text{int}}(t) = \mathbf{F}_{\text{int}}\mathbf{x}_{\text{int}}(t) + \mathbf{B}_{\text{int}}\mathbf{u}(t) + \xi_{\text{int}}(t), \tag{2.1}$$

intended to track a multidimensional process (target)

$$\dot{\mathbf{x}}_{\text{tar}}(t) = \mathbf{F}_{\text{tar}}\mathbf{x}_{\text{tar}}(t) + \xi_{\text{tar}}(t) \tag{2.2}$$

under available measurements

$$\mathbf{z}(t) = \mathbf{H}\mathbf{x}(t) + \xi_{\text{z}}(t), \tag{2.3}$$

the approach yields the optimal control law

$$\mathbf{u}(t) = \mathbf{K}^{-1}\mathbf{B}_{\text{int}}\mathbf{Q}[\hat{\mathbf{x}}_{\text{tar}}(t) - \hat{\mathbf{x}}_{\text{int}}(t)] \tag{2.4}$$

in terms of the minimum value of the performance functional

$$I = M\left\{[\mathbf{x}_{\text{tar}}(t) - \mathbf{x}_{\text{int}}(t)]^{\text{T}}\mathbf{Q}[\mathbf{x}_{\text{tar}}(t) - \mathbf{x}_{\text{int}}(t)] + \int_0^t \mathbf{u}^{\text{T}}(t)\mathbf{K}\mathbf{u}(t)dt\right\}. \tag{2.5}$$

Here, $\mathbf{x}_{\text{int}}$ and $\mathbf{x}_{\text{tar}}$ are the n-dimensional vectors of interceptor and target states, respectively; $\mathbf{F}_{\text{int}}$ and $\mathbf{F}_{\text{tar}}$ are the internal connection matrices of the processes (2.1) and (2.2); $\mathbf{u}$ is the r-dimensional control vector ($r \leqslant n$); $\mathbf{B}_{\text{int}}$ is the control efficiency matrix; $\mathbf{z}$ is the m-dimensional measurement vector ($m \leqslant 2n$); $\mathbf{x} = \left[\mathbf{x}_{\text{tar}}^{\text{T}}\ \mathbf{x}_{\text{int}}^{\text{T}}\right]^{\text{T}}$ is the compound vector; $\mathbf{H}$ is the connection matrix of $\mathbf{z}$

and $\mathbf{x}$; ξ_{int}, ξ_{tar}, and ξ_{mea} are the noise vectors of the states (2.1), (2.2) and measurements (2.3); $\mathbf{Q}$ and $\mathbf{K}$ are **nonnegative definite** penalty matrices for control accuracy and control costs, respectively; t denotes the current control time; $M\{\bullet\}$ is the mathematical expectation given available measurements (2.3); finally, $\hat{\mathbf{x}}_{\text{int}}$ and $\hat{\mathbf{x}}_{\text{tar}}$ are the vectors of the optimal estimates of the processes (2.1) and (2.2), respectively.

In general, the perfection of any control system (its ability to respond to input action changes) is conditioned by the number of feedback loops and the presence of corrective signals. In this case, the number of possible feedback loops is determined by the dimension of the given part (2.1), and the number of corrective signals depends on the dimension of the used input vector (2.2).

In Section 2, we assess the possibility of developing an aircraft guidance method to intensively maneuvering targets based on input signal transformation.

2.1. Control Law Design

In mathematical terms, the design problem is formulated as follows.

Consider an interceptor described by the simplified aircraft model [6]

$$\begin{aligned} &\dot{\varphi}_{\text{int}} = \omega_{\text{int}}, \quad \varphi_{\text{int}}(0) = \varphi_{\text{giv}}, \\ &\dot{\omega}_{\text{int}} = -\frac{1}{T_{\text{int}}}\omega_{\text{int}} + \frac{b}{T_{\text{int}}}u, \quad \omega_{\text{int}}(0) = \omega_{\text{giv}}, \end{aligned} \tag{2.6}$$

intended for a target with a maneuvering law

$$\varphi_{\text{tar}} = f(t), \quad \varphi_{\text{tar}}(0) = \varphi_{\text{tar0}}, \tag{2.7}$$

where $f(t)$ is a smooth, n_{tar} times differentiable function ($n_{\text{tar}} > 2$), and available measurements

$$\varphi_{\text{mea}} = \varphi_{\text{tar}} + \xi_{\text{mea}}. \tag{2.8}$$

For this interceptor, it is required to find a control law u optimizing the performance functional (2.5) and ensuring capture of the target with a complex maneuvering trajectory with changing the sign of the derivative φ_{tar} (2.7) with a miss h not exceeding an admissible threshold h_{adm}.

The expressions (2.6)–(2.8) have the following notation: φ_{tar} and φ_{int} are the target's line-of-sight (LoS) angle and the interceptor's flight direction angle, respectively, with initial values φ_{tar0} and φ_{giv}; ω_{tar} and ω_{int} are the angle rates of the target's LoS and the interceptor's flight direction, respectively, with initial values ω_{tar0} and ω_{giv}; b and T_{int} are the interceptor's gain and time constant, which characterize its dynamic properties; finally, u is the control signal. In formulas (2.6)–(2.8) and below, the time dependence of all variables is omitted for simplicity.

The geometry of the target's and interceptor's angles in the vertical plane is shown in Fig. 1.

In this figure, O_{tar} is the target's location point; $\mathbf{V}_{\text{tar}}$ and $\mathbf{V}_{\text{int}}$ are the velocity vectors of the target and interceptor; φ_{tar} is the target's LoS angle; finally, φ_{int} is the interceptor's flight direction angle.

To realize a complex trajectory of an intercepted object [4], high derivatives of the LoS angle φ_{tar} must be included in its model (2.7).

For the sake of definiteness, we represent the input action (2.7) as the fourth-order vector:

$$\begin{aligned} &\dot{\varphi}_{\text{tar}} = \omega_{\text{tar}}, \quad \varphi_{\text{tar}}(0) = \varphi_{\text{tar0}}, \\ &\dot{\omega}_{\text{tar}} = a_{\text{tar}}, \quad \omega_{\text{tar}}(0) = \omega_{\text{tar0}}, \\ &\dot{a}_{\text{tar}} = \ddot{\omega}_{\text{tar}} = j_{\text{tar}}, \quad a_{\text{tar}}(0) = a_{\text{tar0}}, \\ &\dot{j}_{\text{tar}} = \dddot{\omega}_{\text{tar}} = 0, \quad j_{\text{tar}}(0) = j_{\text{tar0}}, \end{aligned} \tag{2.9}$$

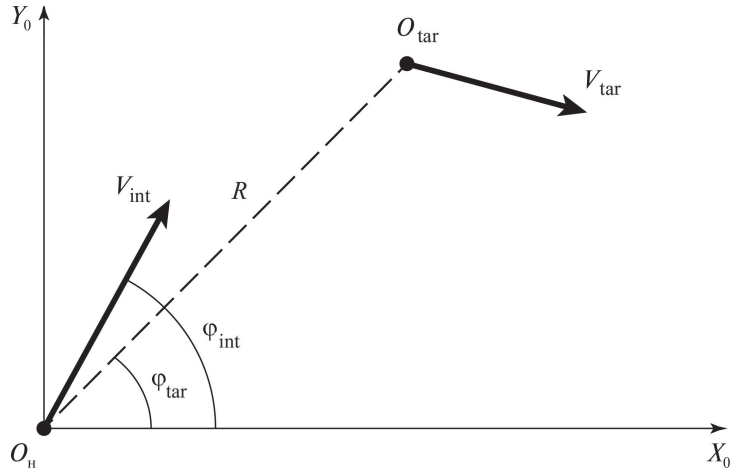

Fig. 1. The mutual arrangement of the target and interceptor in the Cartesian frame.

supplementing the model of the given part (2.6) with the two equations

$$\begin{aligned} \dot{a}_{\text{int}} &= 0, \quad a_{\text{int}}(0) = 0, \\ \dot{j}_{\text{int}} &= 0, \quad j_{\text{int}}(0) = 0. \end{aligned} \tag{2.10}$$

Associating (2.6), (2.10) and (2.9) with (2.1) and (2.2), as applied to (2.5), we obtain

$$\begin{gathered} \mathbf{x}_{\text{tar}} = \begin{bmatrix} \varphi_{\text{tar}} \\ \omega_{\text{tar}} \\ a_{\text{tar}} \\ j_{\text{tar}} \end{bmatrix}, \quad \mathbf{x}_{\text{int}} = \begin{bmatrix} \varphi_{\text{int}} \\ \omega_{\text{int}} \\ 0 \\ 0 \end{bmatrix}, \quad \mathbf{u} = u, \quad \mathbf{B}_{\text{int}} = \begin{bmatrix} 0 \\ b/T_{\text{int}} \\ 0 \\ 0 \end{bmatrix}, \\ \mathbf{Q} = \begin{bmatrix} q_{11} & q_{12} & q_{13} & q_{14} \\ q_{21} & q_{22} & q_{23} & q_{24} \\ q_{31} & q_{32} & q_{33} & q_{34} \\ q_{41} & q_{42} & q_{43} & q_{44} \end{bmatrix}, \quad \mathbf{K} = K_{\text{int}}, \end{gathered} \tag{2.11}$$

where the dimensions of the penalty matrix $\mathbf{Q}$ are extended due to increasing the dimension of the vectors $\mathbf{x}_{\text{int}}$ and $\mathbf{x}_{\text{tar}}$.

Note that the interceptor model (2.6), (2.10) does not correspond to the more complex model of the input action (2.9). Without additional measures, it will execute this action non-optimally.

Using the expressions (2.11) in (2.4), we have

$$u = K_{\text{int}}^{-1} \begin{bmatrix} 0 & \dfrac{b}{T_{\text{int}}} & 0 & 0 \end{bmatrix} \begin{bmatrix} q_{11} & q_{12} & q_{13} & q_{14} \\ q_{21} & q_{22} & q_{23} & q_{24} \\ q_{31} & q_{32} & q_{33} & q_{34} \\ q_{41} & q_{42} & q_{43} & q_{44} \end{bmatrix} \begin{bmatrix} \hat{\varphi}_{\text{tar}} - \hat{\varphi}_{\text{int}} \\ \hat{\omega}_{\text{tar}} - \hat{\omega}_{\text{int}} \\ \hat{\dot{\omega}}_{\text{tar}} - 0 \\ \hat{\ddot{\omega}}_{\text{tar}} - 0 \end{bmatrix},$$

$$u_1 = \frac{bq_{21}}{K_{\text{int}}T_{\text{int}}}(\hat{\varphi}_{\text{tar}} - \hat{\varphi}_{\text{int}}) + \frac{bq_{22}}{K_{\text{int}}T_{\text{int}}}(\hat{\omega}_{\text{tar}} - \hat{\omega}_{\text{int}}) + \frac{bq_{23}}{K_{\text{int}}T_{\text{int}}}\hat{\dot{\omega}}_{\text{tar}} + \frac{bq_{24}}{K_{\text{int}}T_{\text{int}}}\hat{\ddot{\omega}}_{\text{tar}}. \tag{2.12}$$

Direct analysis of (2.12) leads to the following conclusions.

The transformed control signal applied to the interceptor differs from the typical one derived from (2.6) [6]: it contains additional terms with the derivatives of the angle rate, $\hat{\dot{\omega}}_{\text{tar}}$ and $\hat{\ddot{\omega}}_{\text{tar}}$. The weight coefficients of the control errors are determined by the parameters (b/T_{int}) of the given part (2.6), the constraints on the control signal value (K_{int}), and the significance of the individual terms for the entire control signal ($q_{21}, q_{22}, q_{23}, q_{23}$, and q_{24}).

The control signal is represented by a set of terms considering negative feedback loops (their number is determined by the dimension of the model of the given part (2.6)) and corrections (their number depends on the complexity of representing the input actions).

To implement the desired control law, it is necessary to have the estimates $\hat{\varphi}_{\text{tar}}$, $\hat{\omega}_{\text{tar}}$, $\hat{\varphi}_{\text{int}}$, $\hat{\omega}_{\text{int}}$, $\hat{\dot{\omega}}_{\text{tar}}$, and $\hat{\ddot{\omega}}_{\text{tar}}$, which can be generated by different rules [5, 9, 10]. This issue somewhat complicates the tracking system [6] but requires no modifications of the interceptor (2.6), ensuring its optimality in terms of the minimum value of the performance functional (2.5).

Since the interceptor's control law incorporates the higher derivatives $\hat{\dot{\omega}}_{\text{tar}}$ and $\hat{\ddot{\omega}}_{\text{tar}}$, it can track targets with more complex maneuvering laws.

2.2. Analysis of the Effectiveness of the Control Law

The objective of this subsection is to assess the capabilities of the designed control law and its simplified modifications to intercept intensively maneuvering targets.

The effectiveness of the control law (2.12) was analyzed by simulating, in a forward hemisphere, the guidance procedure of the interceptor (2.6) to a target with a complex maneuvering trajectory with changing the sign of the derivatives of its angular coordinates under the perfectly accurate estimates of all the state coordinates φ_{tar}, ω_{tar}, φ_{int}, ω_{int}, $\dot{\omega}_{\text{tar}}$, and $\ddot{\omega}_{\text{tar}}$ used in (2.6).

During the simulation process, three modifications of control laws (with different degrees of interceptor's adaptation to the input actions) were compared for (2.6) as follows:

$$u_1 \text{ given by (2.12)},$$

$$u_2 = \frac{bq_{21}}{K_{\text{int}}T_{\text{int}}}(\hat{\varphi}_{\text{tar}} - \hat{\varphi}_{\text{int}}) + \frac{bq_{22}}{K_{\text{int}}T_{\text{int}}}(\hat{\omega}_{\text{tar}} - \hat{\omega}_{\text{int}}) + \frac{bq_{23}}{K_{\text{int}}T_{\text{int}}}\hat{\dot{\omega}}_{\text{tar}}, \tag{2.13}$$

$$u_3 = \frac{bq_{21}}{K_{\text{int}}T_{\text{int}}}(\hat{\varphi}_{\text{tar}} - \hat{\varphi}_{\text{int}}) + \frac{bq_{22}}{K_{\text{int}}T_{\text{int}}}(\hat{\omega}_{\text{tar}} - \hat{\omega}_{\text{int}}). \tag{2.14}$$

The effectiveness of guidance was evaluated by the current miss rate $h = R^2\omega_{\text{tar}}/V_{\text{o}}$, where R and V_{o} are the target's range and relative speed, respectively, under different time constants T_{int}.

Figures 2 and 3 show the trajectories of the target (T) and interceptor (I) controlled by the laws (2.12), (2.13), (2.14) (in one of the modifications) as well as the corresponding final and current miss rates. The dots indicate the positions of the target and interceptors at the same time instants.

According to the figures, the classical guidance method (2.14) does not ensure the interception of the intensively maneuvering target whereas the laws (2.12), (2.13) implement high-accuracy interception.

Based on the simulation results, we draw several conclusions:

- For the target's flight trajectory under analysis, in order to improve guidance accuracy, including $\dot{\omega}_{\text{tar}}$ in the control law (2.12) is more important than including $\ddot{\omega}_{\text{tar}}$.
- Using more inertial interceptors ($T_{\text{int2}} = 2T_{\text{int1}}$) slightly increases misses for the control laws (2.12), (2.13) and significantly increases misses for the control law (2.14).
- Similar results are observed when increasing the target's speed ($V_{\text{tar2}} = 2V_{\text{tar1}}$).

The simulation confirmed the effectiveness of the proposed guidance system optimization method based on transforming the input action in a wide range of target's speeds and interceptor's delays.

By manipulating the original models (2.7), (2.9), the penalty matrices $\mathbf{Q}$ and $\mathbf{K}$ in (2.5), (2.11), and the nature of their variation in time, one can obtain a large set of guidance methods that satisfy, to a greater or lesser extent, the requirements listed in part I of the study; for details, see [7].

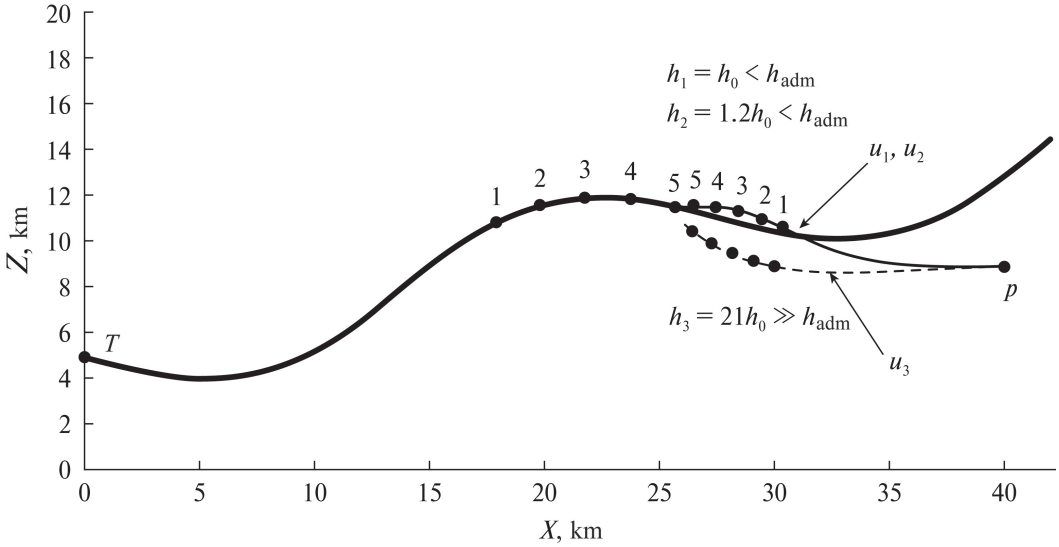

Fig. 2. The trajectories of the target and interceptors.

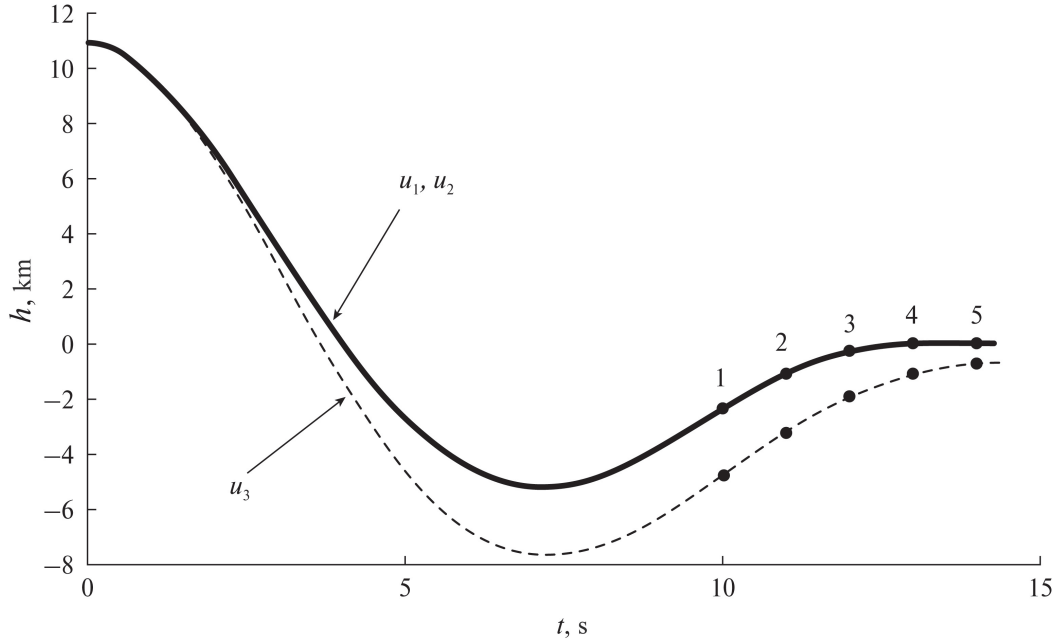

Fig. 3. Current miss rate depending on time.

As a disadvantage of this optimization method, we note the need to estimate the derivatives of the angular rate, which represents a nontrivial problem. One solution was proposed in [6].

3. GUIDANCE OPTIMIZATION BASED ON PREDICTING THE SPATIAL POSITION OF THE TARGET

In Section 2, we have discussed an optimization approach based on adapting the guidance method to a particular interceptor type, which significantly reduces the cost of developing an HSA interception system. However, another approach is also possible: adapt an interceptor to a particular guidance method without changing its dynamic properties.

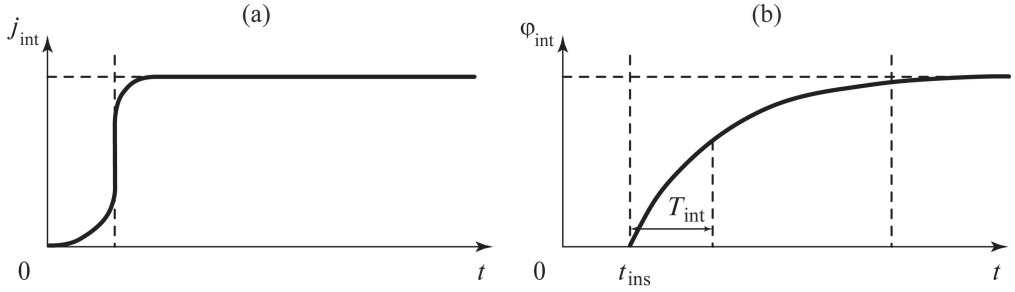

Fig. 4. (a) The input action depending on time and (b) the response to this action.

Here, the core is to compensate, by a certain method, for the delay of the interceptor's response to the control action caused by its inertia and insensitivity zone.

In Fig. 4, these features are qualitatively illustrated by the presence of the insensitivity zone t_{ins}, which determines the delay of the interceptor's response to a small control signal (see Fig. 4a), and the time constant T_{int} (see Fig. 4b) in the process of changing the interceptor's flight direction under the action of the control signal j_{int}.

The delay in the interceptor's response to a control action can be compensated for in various ways. One method is based on including the mismatch between the dynamic properties of the target and interceptor in the control law [6]. However, it is effective only at short distances to the target. In the second, control errors are formed not by the target's current position but by its prediction for a known delay in the interceptor's execution of control signals. This method can be used throughout the entire guidance procedure.

Both approaches can be (quite simply) realized within the local STOC under measured disturbances [5].

Consider the general case of this framework. For a given system (interceptor) described by

$$\dot{\mathbf{x}}_{\text{int}}(t) = \mathbf{F}_{\text{int}}\mathbf{x}_{\text{int}}(t) + \mathbf{B}_{\text{int}}\mathbf{u}(t) + \mathbf{s}_{\text{int}}(t) + \xi_{\text{int}}(t), \quad \mathbf{x}_{\text{int}}(0) = \mathbf{x}_{\text{int}0}, \tag{3.1}$$

intended to track a multidimensional process (target)

$$\dot{\mathbf{x}}_{\text{tar}}(t) = \mathbf{F}_{\text{tar}}\mathbf{x}_{\text{tar}}(t) + \xi_{\text{tar}}(t), \quad \mathbf{x}_{\text{tar}}(0) = \mathbf{x}_{\text{int}0}, \tag{3.2}$$

under available measurements

$$\mathbf{z}(t) = \mathbf{H}\left[\mathbf{x}_{\text{tar}}^{\text{T}}(t) \quad \mathbf{x}_{\text{int}}^{\text{T}}(t)\right]^{\text{T}} + \xi_{\text{z}}(t), \tag{3.3}$$

the local STOC yields the optimal control law

$$\mathbf{u}(t) = \mathbf{K}^{-1}\mathbf{B}_{\text{int}}^{\text{T}}\left[Q\left(\hat{\mathbf{x}}_{\text{tar}}(t) - \hat{\mathbf{x}}_{\text{int}}(t)\right) - \mathbf{G}\hat{\mathbf{s}}_{\text{int}}(t)\right] \tag{3.4}$$

in terms of the minimum value of the performance functional

$$I = M\left\{\Delta\mathbf{x}^{\text{T}}(t)\mathbf{Q}\Delta\mathbf{x}(t) + 2\Delta\mathbf{x}^{\text{T}}(t)\mathbf{G}\mathbf{s}_{\text{int}}(t) + \mathbf{s}_{\text{int}}^{\text{T}}(t)\mathbf{Q}\mathbf{s}_{\text{int}}(t) + \int_0^t \mathbf{u}^{\text{T}}(t)\mathbf{K}\mathbf{u}(t)dt\right\}, \tag{3.5}$$

$$\Delta\mathbf{x}(t) = \mathbf{x}_{\text{tar}}(t) - \mathbf{x}_{\text{int}}(t). \tag{3.6}$$

Here, $\mathbf{s}_{\text{int}}$ and $\hat{\mathbf{s}}_{\text{int}}$ are the n-dimensional vectors of measured disturbances and their optimal estimates; $\mathbf{G}$ is a nonnegative definite penalty matrix of the disturbances.

The objective of Section 3 is to assess the possibility of using the apparatus (3.1)–(3.6) to develop HSA interception methods.

3.1. Control Law Design

In mathematical terms, the design problem is formulated as follows. For a system described by

$$\begin{aligned} \dot{\varphi}_{\text{int}}(t) &= \omega_{\text{int}}(t), & \varphi_{\text{int}}(0) &= \varphi_{\text{int}0}, \\ \dot{\omega}_{\text{int}}(t) &= -\frac{1}{T_{\text{int}}}\omega_{\text{int}}(t) + \frac{b}{T_{\text{int}}}j_{\text{int}}(t), & \omega_{\text{int}}(0) &= \omega_{\text{int}0}, \end{aligned} \tag{3.7}$$

intended to intercept an HSA by predicting its spatial position for a time T_{pre} :

$$\begin{aligned} \dot{\varphi}_{\text{tar}}(t+T_{\text{pre}}) &= \omega_{\text{tar}}(t) + \dot{\omega}_{\text{tar}}(t)T_{\text{pre}}, \qquad \varphi_{\text{tar}}(0) = \varphi_{\text{tar}}(T_{\text{pre}}), \\ \dot{\omega}_{\text{tar}}(t+T_{\text{pre}}) &= -\frac{2\dot{R}(t)}{R(t)}\omega_{\text{tar}}(t) + \frac{1}{R(t)}(j_{\text{tar}}(t) - j_{\text{int}}(t)) + \ddot{\omega}_{\text{tar}}(t)T_{\text{pre}}, \\ & \qquad \omega_{\text{tar}}(0) = \omega_{\text{tar}}(T_{\text{pre}}), \end{aligned} \tag{3.8}$$

it is required to find a control signal j_{int} optimizing the performance functional

$$\begin{aligned} I = M\Bigg\{ & \begin{bmatrix} \Delta\varphi \\ \Delta\omega \end{bmatrix}^{\text{T}} \begin{bmatrix} q_{11} & q_{12} \\ q_{21} & q_{22} \end{bmatrix} \begin{bmatrix} \Delta\varphi \\ \Delta\omega \end{bmatrix} + 2 \begin{bmatrix} \Delta\varphi \\ \Delta\omega \end{bmatrix}^{\text{T}} \begin{bmatrix} g_{11} & g_{12} \\ g_{21} & g_{22} \end{bmatrix} \\ & \times \begin{bmatrix} \dot{\omega}_{\text{tar}}T_{\text{pre}} \\ \left(\dfrac{1}{T_{\text{int}}} - \dfrac{2\dot{R}}{R}\right)\omega_{\text{tar}} + \ddot{\omega}_{\text{tar}}T_{\text{pre}} \end{bmatrix} + \begin{bmatrix} \dot{\omega}_{\text{tar}}T_{\text{pre}} \\ \left(\dfrac{1}{T_{\text{int}}} - \dfrac{2\dot{R}}{R}\right)\omega_{\text{tar}} + \ddot{\omega}_{\text{tar}}T_{\text{pre}} \end{bmatrix}^{\text{T}} \\ & \times \begin{bmatrix} q_{11} & q_{12} \\ q_{21} & q_{22} \end{bmatrix} \begin{bmatrix} \dot{\omega}_{\text{tar}}T_{\text{pre}} \\ \left(\dfrac{1}{T_{\text{int}}} - \dfrac{2\dot{R}}{R}\right)\omega_{\text{tar}} + \ddot{\omega}_{\text{tar}}T_{\text{pre}} \end{bmatrix} + \int_0^t j_{\text{int}}^2 K_{\text{int}}\,dt \Bigg\}. \end{aligned} \tag{3.9}$$

The geometry of the target's and interceptor's angles is shown in Fig. 3.1.

In formula (3.9) and below, the time dependence of all variables is omitted for simplicity.

Using (3.7) and (3.8) in (3.6), we derive the system of equations

$$\begin{aligned} \Delta\dot{\varphi} &= \dot{\varphi}_{\text{tar}} - \dot{\varphi}_{\text{int}} = \Delta\omega + \dot{\omega}_{\text{tar}}T_{\text{pre}}, \\ \Delta\dot{\omega} &= \dot{\omega}_{\text{tar}} - \dot{\omega}_{\text{int}} = -\frac{1}{T_{\text{int}}}\Delta\omega - \frac{b}{T_{\text{int}}}j_{\text{int}} + \frac{1}{T_{\text{int}}}\omega_{\text{tar}} + \dot{\omega}_{\text{tar}} + \ddot{\omega}_{\text{tar}}T_{\text{pre}}. \end{aligned} \tag{3.10}$$

Therefore, the mismatch between the dynamic properties of the target and interceptor (acting as a measured disturbance) is given by the vector [5]

$$\mathbf{s}_{\text{int}} = \begin{bmatrix} \dot{\omega}_{\text{tar}}T_{\text{pre}} \\ \left(\dfrac{1}{T_{\text{int}}} - \dfrac{2\dot{R}}{R}\right)\omega_{\text{tar}} + \ddot{\omega}_{\text{tar}}T_{\text{pre}} \end{bmatrix}. \tag{3.11}$$

Using (3.10) and (3.11) in (3.4), we obtain

$$\begin{aligned} j_{\text{int}} = \frac{1}{K_{\text{int}}} & \begin{bmatrix} 0 & \dfrac{b}{T_{\text{int}}} \end{bmatrix} \Bigg\{ \begin{bmatrix} q_{11} & q_{12} \\ q_{21} & q_{22} \end{bmatrix} \begin{bmatrix} \Delta\hat{\varphi} \\ \Delta\hat{\omega} \end{bmatrix} - \begin{bmatrix} g_{11} & g_{12} \\ g_{21} & g_{22} \end{bmatrix} \begin{bmatrix} \hat{\dot{\omega}}_{\text{tar}}T_{\text{pre}} \\ \left(\dfrac{1}{T_{\text{int}}} - \dfrac{2\hat{\dot{R}}}{\hat{R}}\right)\hat{\omega}_{\text{tar}} + \hat{\ddot{\omega}}_{\text{tar}}T_{\text{pre}} \end{bmatrix} \Bigg\}, \\ j_{\text{int}} = {} & \frac{bq_{21}}{K_{\text{int}}T_{\text{int}}}\Delta\hat{\varphi} + \frac{bq_{22}}{K_{\text{int}}T_{\text{int}}}\Delta\hat{\omega} + \frac{bg_{22}}{K_{\text{int}}T_{\text{int}}}\left(\frac{1}{T_{\text{int}}} - \frac{2\hat{\dot{R}}}{\hat{R}}\right)\hat{\omega}_{\text{tar}} \\ & + \frac{bg_{21}}{K_{\text{int}}T_{\text{int}}}\hat{\dot{\omega}}_{\text{tar}}T_{\text{pre}} + \frac{bg_{22}}{K_{\text{int}}T_{\text{int}}}\hat{\ddot{\omega}}_{\text{tar}}T_{\text{pre}}. \end{aligned} \tag{3.12}$$

Direct analysis of (3.12) leads to the following conclusions.

1. If $V_{\text{int}} > V_{\text{tar}}$, this method is all-sector and all-altitude. All-sector interception is provided by considering the signs of angular errors, the LoS and angle rate, and its derivatives. All-altitude interception is provided by using transverse acceleration as a control signal (instead of rudders, whose effectiveness depends on air density (altitude)).

2. Including the derivatives $\dot{\omega}_{\text{tar}}$ and $\ddot{\omega}_{\text{tar}}$ of the LoS angle rate in the control law allows guiding to intensively maneuvering targets.

3. The significance of the last three terms grows with approaching the target and increasing the forecast time.

4. To implement this guidance law, one needs optimal estimates of the range, approach speed, relative bearing, LoS angle rate, and its derivatives [5, 10, 11].

3.2. Analysis of the Effectiveness of the Control Law

The objective of this subsection is to assess the capabilities of the control law (3.12) and its simplified modifications to intercept intensively maneuvering targets.

The effectiveness of this law was analyzed by simulating, in a forward hemisphere, the guidance procedure of the interceptor (3.7) to the target (3.8) with a complex maneuvering trajectory with changing the sign of the derivatives of its angular coordinates under the perfectly accurate estimates of all the state coordinates and $V_{\text{int}} < V_{\text{tar}}$.

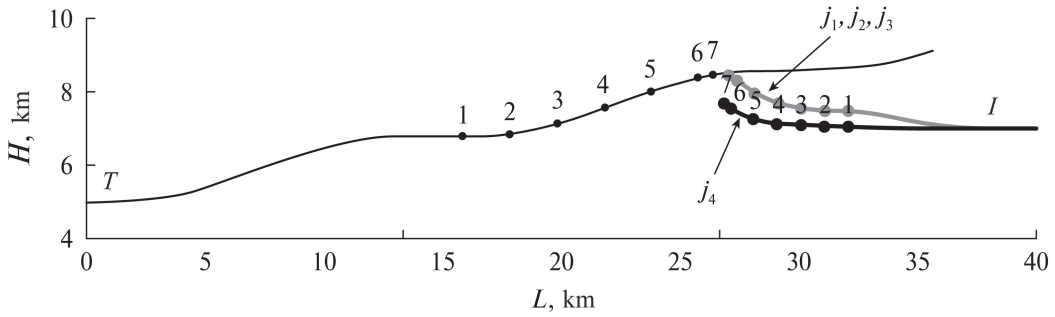

Fig. 5. The trajectories of the target and interceptors with different guidance laws.

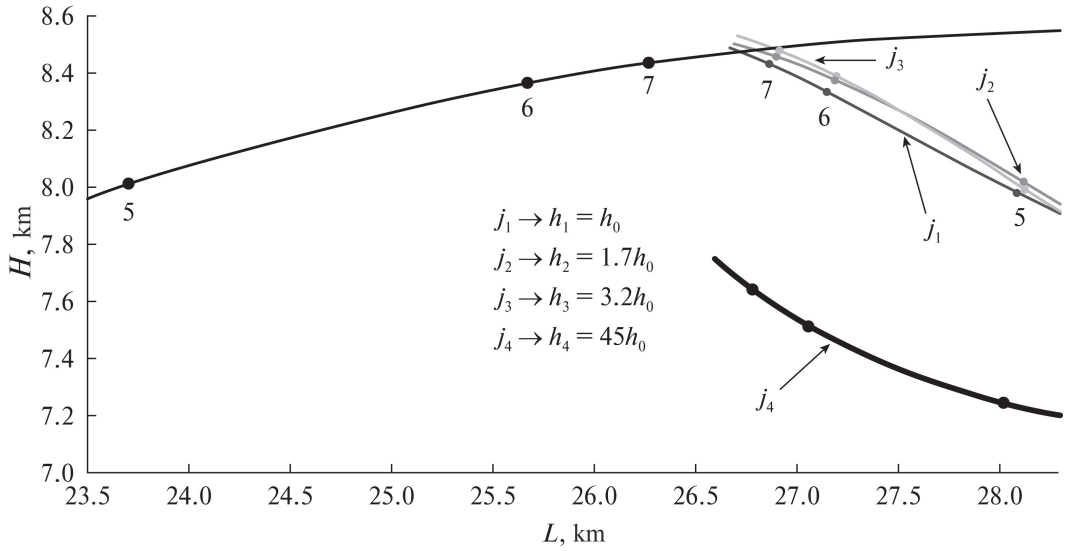

Fig. 6. The final section of the target's and interceptor's trajectories.

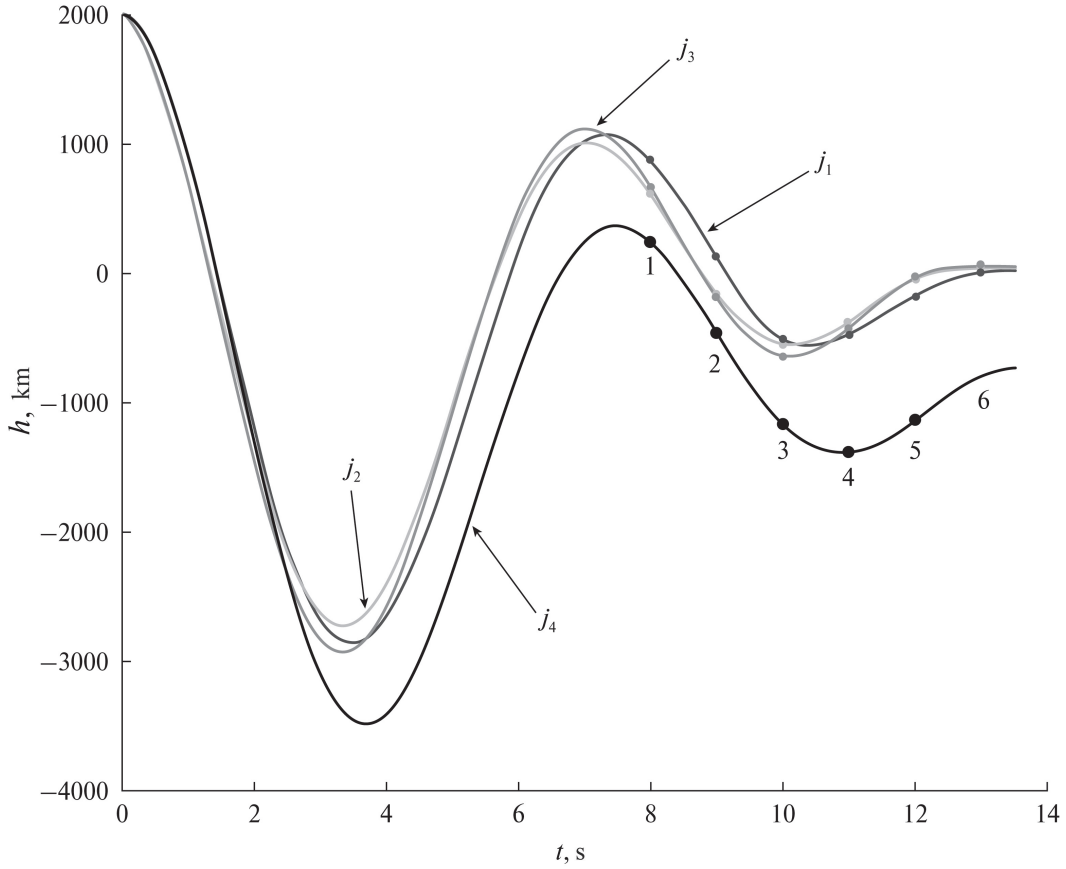

Fig. 7. The current miss rates of interceptors.

During the simulation process, four modifications of control laws were compared as follows:

$$j_1 \text{ given by (3.12)},$$

$$j_2 = \frac{bq_{21}}{K_{\text{int}}T_{\text{int}}}\Delta\hat{\varphi} + \frac{bq_{22}}{K_{\text{int}}T_{\text{int}}}\Delta\hat{\omega} + \frac{bg_{22}}{K_{\text{int}}T_{\text{int}}}\left(\frac{1}{T_{\text{int}}} - \frac{2\hat{\dot{R}}}{\hat{R}}\right)\hat{\omega}_{\text{tar}} + \frac{bg_{21}}{K_{\text{int}}T_{\text{int}}}\hat{\dot{\omega}}_{\text{tar}}T_{\text{pre}},$$

$$j_3 = \frac{bq_{21}}{K_{\text{int}}T_{\text{int}}}\Delta\hat{\varphi} + \frac{bq_{22}}{K_{\text{int}}T_{\text{int}}}\Delta\hat{\omega} + \frac{bg_{22}}{K_{\text{int}}T_{\text{int}}}\left(\frac{1}{T_{\text{int}}} - \frac{2\hat{\dot{R}}}{\hat{R}}\right)\hat{\omega}_{\text{tar}},$$

$$j_4 = \frac{bq_{21}}{K_{\text{int}}T_{\text{int}}}\Delta\hat{\varphi} + \frac{bq_{22}}{K_{\text{int}}T_{\text{int}}}\Delta\hat{\omega}.$$

The effectiveness of guidance was evaluated by the current and final miss rates and the control signal value under different time constants T_{int} and prediction times T_{pre}.

Figures 5 and 6 show the trajectories of the target (T) and interceptors (I) with the control laws j_1–j_4; points 1–5 indicates their current positions. Figures 7 and 8 present the corresponding miss rates and accelerations.

Based on the simulation results, we draw several conclusions:

1. The control laws with the signals j_1–j_3 realize a sufficiently high accuracy, which decreases with excluding individual terms. The conventional guidance method with the signal j_4 does not ensure the interception of an intensively maneuvering HSA (with changing the sign of the derivatives of its angular coordinates).

2. Guidance accuracy deteriorates when increasing the interceptor's delay.

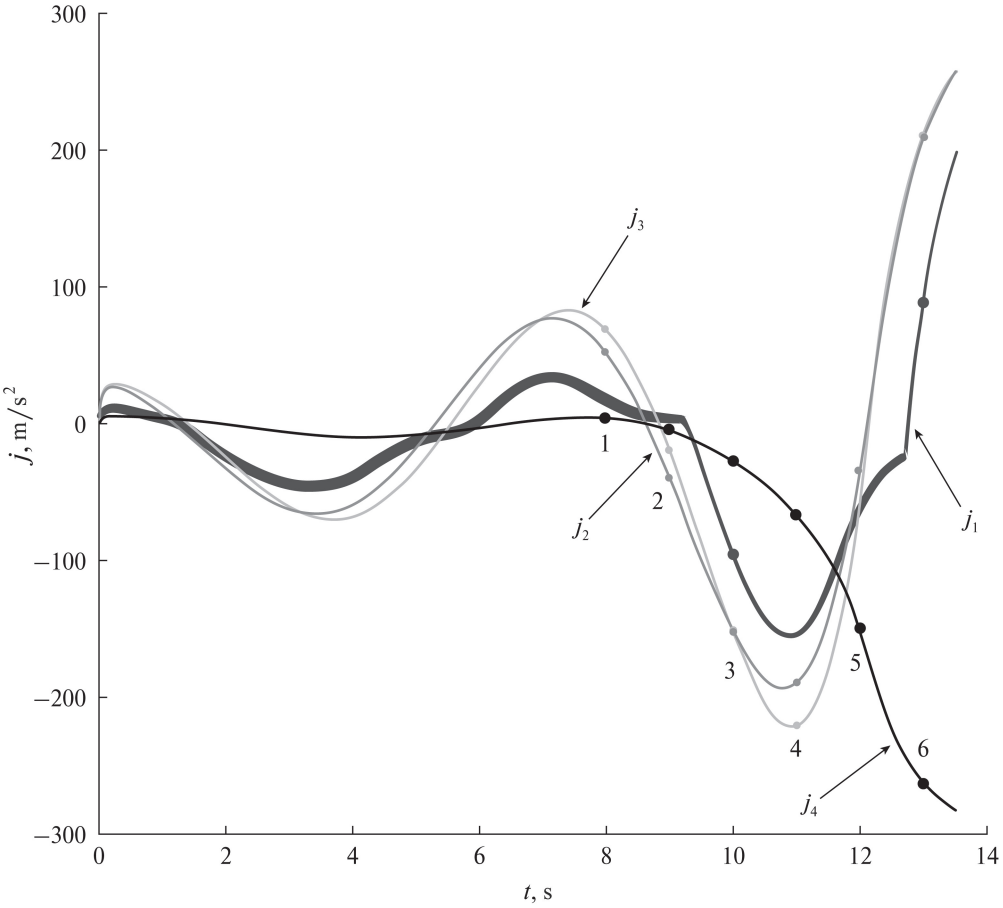

Fig. 8. The graphs of control signals.

3. Increasing the prediction time to $T_{\text{pre}} = 2T_{\text{int}}$ improves guidance accuracy.

4. Guidance is performed within the realizable transverse accelerations.

As a disadvantage, we note the complexity of information support due to the need to estimate the derivatives of the LoS angle rate.

4. CONCLUSIONS

The material presented in this paper leads to the following findings.

The mathematical apparatus of local STOC optimization can be used to develop guidance methods to HSA considering the carrier's dynamic properties. The problem can be solved by at least two approaches.

The first is based on transforming input actions. It provides adaptation of the guidance method and its information support to a particular carrier type.

Within the second approach, the control signal is formed by predicting the target's position for a time determined by the carrier's inertia (instead of the current state of the interceptor and target). Both approaches do not require redesigning the carrier to improve its maneuverability, which significantly reduces the cost of developing an interceptor system.

Both approaches ensure the interception of an intensively maneuvering HSA by including the derivatives of the angle rate in guidance methods. This will require complicating somehow the angular measurement channel of the onboard radar system.

REFERENCES

1. *Aviatsionnye sistemy radioupravleniya* (Aircraft Radio Control Systems), Merkulov, V.I., Ed., Moscow: Zhukovsky Air Force Engineering Academy, 2008.
2. Girard, A.R. and Kabamba, P.T., Proportional Navigation: Optimal Homing and Optimal Evasion, *SIAM Review*, 2015, vol. 57, no. 4, pp. 611–624.
3. An, JY., Lee, CH., and Tahk, MJ., A Collision Geometry-Based Guidance Law for Course-Correction-Projectile, *Int. J. Aeronaut. Space Sci.*, 2019, vol. 20, no. 2, pp. 442–458.
4. Verba, V.S., Merkulov, V.I., Zakomoldin, D.V., and Likhachev, V.P., Problems of Interception of High Speed Aircraft Maneuvering According to Complex Laws. Part 2. Analysis of Flight Paths of Foreign Aircraft, *Achievements of Modern Radioelectronics*, 2024, vol. 78, no. 4, pp. 5–14.
5. Merkulov, V.I. and Verba, V.S., *Sintez i analiz aviatsionnykh radioelektronnykh sistem upravleniya. Kniga 1* (Design and Analysis of Aircraft Radioelectronic Control Systems. Book 1), Moscow: Radiotekhnika, 2023.
6. Merkulov, V.I. and Verba, V.S., *Sintez i analiz aviatsionnykh radioelektronnykh sistem upravleniya. Kniga 2* (Design and Analysis of Aircraft Radioelectronic Control Systems. Book 2), Moscow: Radiotekhnika, 2023.
7. Verba, V.S. and Merkulov, V.I., Approaches to Optimizing Guidance Methods to High-Speed Intensively Maneuvering Targets. Part I. Justifying Requirements for Ways to Optimize Guidance Methods, *Autom. Remote Control*, 2024, vol. 85, no. 11, pp. 1108–1112.
8. Galyaev, A.A., Lysenko, P.V., and Rubinovich, E.Y., Optimal Stochastic Control in the Interception Problem of a Randomly Tracking Vehicle, *Mathematics*, 2021, vol. 9, no. 19, art. no. 2386.
9. Su, W., Li, K., and Chen, L., Coverage-Based Cooperative Guidance Strategy against Highly Maneuvering Target, *Aerospace Science and Technology*, 2017, vol. 71, pp. 147–155.
10. Song, F., Y. Li, Y., Cheng, W., et al., An Improved Kalman Filter Based on Long Short-Memory Recurrent Neural Network for Nonlinear Radar Target Tracking, *Wireless Communications and Mobile Computing*, 2022, no. 7, pp. 1–10.
11. Prokhorov, M.B. and Saul'ev, V.K., The Kalman–Bucy Method of Optimal Filtering and Its Generalizations, *Journal of Soviet Mathematics*, 1979, vol. 12, no. 3, pp. 354–380.

This paper was recommended for publication by A.A. Galyaev, a member of the Editorial Board